Q. J. R. Meteorol. Soc. (1995), **121**, pp. 631–654 551.509.327:551.509.313.4

Data sparsity and the tropical-cyclone analysis and prediction problem: Some simulation experiments with a barotropic numerical model

By HARRY C. WEBER* and ROGER K. SMITH
University of Munich, Germany

(Received 17 November 1993; revised 3 October 1994)

SUMMARY

Some simulation experiments relevant to the problem of determining the minimum data requirements for the accurate reconstruction of tropical-cyclone-scale vortices from given sparse data distributions are described. Also, the accuracy with which the vortex track can be predicted using these data is investigated. The experiments are based on a 96-hour numerical integration of the barotropic vorticity equation on a beta-plane, starting with a symmetric tropical-cyclone-scale vortex embedded in zonal shear flow. After 48 hours, when asymmetries in the vortex circulation have developed, the model fields in this 'control' calculation are used as a 'perfect' data set to assess the analysis strategy described. The 20 km horizontal resolution of these new initial data is progressively degraded to test the ability of the analysis procedure to reconstruct the perfect analysis. The analyses of the degraded data sets are used as an initial condition for a further 48-hour integration of the model, and the resulting vortex tracks are compared with that in the second half of the control run. The influence of the analysed vortex asymmetry on the subsequent vortex track is also studied.

As the resolution of the simulated initial data is degraded, so is the information that these data provide on the symmetric circulation and the vortex-induced asymmetries, and ultimately it becomes necessary to introduce 'synthetic' data in the analysis. The calculations indicate some of the problems that need to be overcome to introduce such data properly.

The analysis method provides a general way to partition the flow into four components: the large-scale environment, the symmetric vortex, the vortex asymmetry, and the small-scale environment. The large-scale environment is characterized by the lowest few wave numbers in a two-dimensional Fourier analysis. The residual field is subjected to an azimuthal Fourier analysis about the cyclone centre, and the last three components of the partition are defined by the symmetric component, the wave-number-one component and the sum of all higher wave-number components of this analysis, respectively. An attractive feature of such a partition is that the total flow across the centre of the symmetric vortex, which governs the vortex motion in a barotropic model, is contained in only two components: the large-scale environment and the vortex asymmetry.

1. INTRODUCTION

Tropical cyclones form and mature over the tropical oceans where the density of meteorological observing stations is relatively low, especially upper-air stations. Indeed, were it not for satellite surveillance, it would be possible for storms in some locations to go completely undetected by the conventional data network. While satellite data are limited in their ability to replace surface observations and upper-air soundings, satellite imagery enables cyclones to be tracked, and satellite-derived cloud-drift winds at upper and lower tropospheric levels can provide useful information about the airflow in the cyclone environment. Despite such measurements, the overall paucity of data in and around tropical cyclones appears to be a significant factor in the difficulty of accurately predicting their track, even for one or two days in advance. The situation is still such that operational analysis schemes may not recognize the existence of a particular storm, or may place it in the wrong location. As an example, the operational analysis and prediction scheme of the European Centre for Medium-range Weather Forecasts (ECMWF) did not recognize the existence of Hurricane Andrew in 1992 until shortly before the storm made landfall in southern Florida, although the model's overall per-

* Corresponding author: Meteorological Institute, University of Munich, Theresienstr. 37, 80333 Munich, Germany.

formance is usually remarkably good (M. J. Miller, personal communication). Insufficient resolution of a storm in numerical forecast models may compromise the quality of track predictions also.

Hurricanes that threaten the United States of America are frequently monitored by surveillance and research aircraft which supplement conventional observations with dropsonde soundings in and around the storm and provide information on its intensity. However, for storms that occur elsewhere such data are unavailable, and intensity estimates are based on the interpretation of satellite imagery. Even with aircraft observations it is usually necessary to incorporate a 'synthetic vortex' or 'synthetic observations' in an analysis to obtain a sufficiently well positioned and well structured representation of an existing cyclone to enable the future storm movement to be forecast with any accuracy. Sometimes the synthetic vortex is based on fields derived from an axisymmetric model vortex, possibly generated by spinning-up a cyclone in an axisymmetric version of the forecast model (Hovermale and Livezey 1977), or it is simply an analytically prescribed symmetric-vortex profile (Iwasaki *et al.* 1987; Andersson and Hollingsworth 1988). In other cases, asymmetries have been included in the specification of the synthetic vortex in an attempt to ensure that the predicted initial motion is consistent with the recent observed motion of the storm before the analysis time (e.g. Mathur 1991; Davidson and Puri 1992). Generally, the effectiveness of such schemes has been assessed in terms of their performance in improving the predicted tracks of a series of individual storms. While there is a gradual overall trend towards better forecasts of hurricane tracks, there remain many individual cases where the track prediction is relatively poor. This variation in skill may be due to a number of factors, including the method used to prescribe a synthetic vortex in a particular case. In this paper we try to develop a methodology for identifying some of the analysis problems.

In the last few years, theories of tropical-cyclone motion have advanced considerably, especially within a barotropic context (see, for example, the review by Smith (1993)). Ulrich and Smith (1991) have shown that the motion of a barotropic vortex is determined approximately by the vector sum of the environmental flow at the vortex centre and the asymmetric flow there. The latter is induced by the vortex itself as it distorts the ambient absolute-vorticity field in its neighbourhood. This distortion leads *inter alia* to an azimuthal wave-number-one pattern of relative vorticity about the vortex centre, and the flow associated with this has an important influence on the motion of the vortex. Although considerable skill has been achieved during the last few years in forecasting tropical-cyclone tracks without much realism of the symmetric vortex and the vortex asymmetries, it is reasonable to expect that a more realistic representation of these features in the initial fields of numerical prediction models would lead to a further improvement of track prognoses (cf. Kurihara *et al.* 1993). With this in mind, we outline a systematic approach for the evaluation or development of a vortex-enhancement scheme. This scheme should provide as much information as possible about the structure of the vortex environment, the symmetric vortex, and the vortex asymmetries from sparsely distributed meteorological data. The method described in this paper may be useful also to evaluate the accuracy of the foregoing partitioning components in data fields resulting from other vortex-enhancement schemes.

Operational forecast models like the Tropical Analysis and Prediction System (TAPS) of the Australian Bureau of Meteorology Research Centre (see Davidson and Puri 1992) can be run at a relatively high resolution (e.g. 50 km horizontal grid size), thereby allowing a better representation of tropical cyclones than is usually the case. However, in order to exploit this capability fully, there remains the problem of finding a suitable method to analyse the storm and its environment from a mostly inadequate data set, and then a method to use this information to construct a synthetic vortex that is as realistic as possible to initialize the forecast model. The former task provides the main focus of the present paper and we concentrate on aspects of the problem that can be addressed using a barotropic model. We study also the accuracy of the subsequent vortex-track forecasts in relation to our analyses.

The present paper is seen as an extension of the study of Reeder *et al.* (1991) who explored the resolution required to resolve adequately the vortex asymmetry that is associated with hurricane motion. The idea is to use a simulated, high-resolution data set to assess the scientific basis of our analysis strategy. The data, with a uniform horizontal resolution of 20 km, were created using the numerical model described by Ulrich and Smith (1991). Observational data against which such strategies may be tested do not approach anywhere near this resolution, even when supplemented by airborne dropsonde soundings. A complete knowledge of the actual structure of the initial data enables one to assess the maximum information that can be extracted from progressively degraded subsets of these.

In detail the method is as follows. First we carry out a numerical integration of the barotropic vorticity equation on a beta-plane in which there is an imposed large-scale zonal shear flow. At the initial time, a symmetric tropical-cyclone-scale vortex is inserted in the flow and the integration is carried out for a period of 96 hours. Thereby, the evolution of the flow and, in particular, the vortex track can be determined with precision using a high-resolution grid for the calculation. As already described, the vortex circulation interacts with the large-scale environment in its vicinity, and asymmetries develop in the vorticity field. At some given time, say after 48 hours of integration, the high-resolution data are taken as a simulated data set which can be subjected to an analysis and used as an initial condition for a further 48-hour integration. Our strategy will be to degrade the resolution of the simulated data progressively by sampling it on coarser and coarser grids. Following this we carry out an analysis of the degraded data, interpolate it to the original fine grid and restart the integration. For each set of degraded data, some of which differ substantially from each other (especially those with low resolution), we study the degree of deterioration in the vortex and mean-flow structure in the analysis as a function of the amount of degradation. The quality of the analysis is assessed also by using it to predict the vortex track for the subsequent 48 hours, which is compared with the track in the control calculation. In particular we investigate: (i) the possibilities and problems connected with the initial positioning of the vortex, (ii) the deterioration of the track forecast with decreasing resolution, and (iii) the relative importance of the analysed vortex asymmetries on the vortex track. Furthermore we describe an accurate method for determining the vortex centre if the initial data are not too sparse. Finally we consider the problems of introducing a synthetic vortex into the analysis when the degraded data are so coarse that they contain insufficient information about the original vortex to be of use in the re-initialization of the numerical model. This corresponds with the usual situation in the atmosphere, where, in addition, the data are irregularly distributed. This irregularity is a major obstacle for an accurate analysis because the data have to be processed on to a regular grid and suffer aliasing when interpolated on to this.

In sections 2, 3 and 4 we present briefly the details of our analysis and introduce the techniques applied to partition a particular data field into suitable components. We discuss also some problems related to these techniques. The results of our experiments are presented in section 5 and discussed in section 6 together with an overview of the future work necessary to improve the construction of synthetic vortices and therewith the prediction of tropical-cyclone motion in barotropic models.

2. The simulated vortex data

(a) The basic data set

The simulated data fields for the subsequent analysis are obtained by a numerical integration of the nondivergent barotropic vorticity equation on a beta-plane centred at 12.5° latitude. The calculation is similar to one described by Ulrich and Smith (1991) in which the initial state consists of a symmetric vortex imposed on a zonal environmental flow. A relatively large domain size of 5000 km is chosen in both the x (eastward) and y (northward) direction to minimize boundary effects. Rigid walls are imposed at the northern and southern boundary of the domain, while the boundary conditions on the eastern and western end of the domain are assumed to be periodic.

The zonal flow is specified by its stream function which has the form

$$\psi_E = \psi_{E0} \cos\left(\frac{\pi y}{L}\right) \tag{2.1}$$

where L denotes the domain size and $\psi_{E0} = 10L/\pi$.

The narrow profile used by Smith and Ulrich (1990) is chosen for the initial symmetric vortex; this has a maximum tangential velocity of 40 m s^{-1} at a radius r_m of 100 km and a region of gale-force winds (wind speed greater than 15 m s^{-1}) that extends to a radius of 235 km from the vortex centre. The vortex stream function is given by the formula

$$\psi_V(s) = -\frac{\psi_0}{1 + as^2 + bs^6} \tag{2.2}$$

where $\psi_0 = 7.9049 \times 10^6$ m^{2}s^{-1}, $a = 0.52176$ and $b = 2.8859 \times 10^{-2}$. The nondimensional radius $s = r/r_m$, where r is the dimensional radius measured from the centre of the vortex.

Figure 1 shows cross-sections of the total stream function $\psi_E + \psi_V$ and total vorticity $\zeta_E + \zeta_V$ in the y direction at the initial time together with those of the environmental stream function and vorticity, ψ_E and ζ_E. It should be noted that the magnitude of the vortex stream function at large radii is rather small compared with that of the environmental stream function, whereas the corresponding relative vorticity derived from

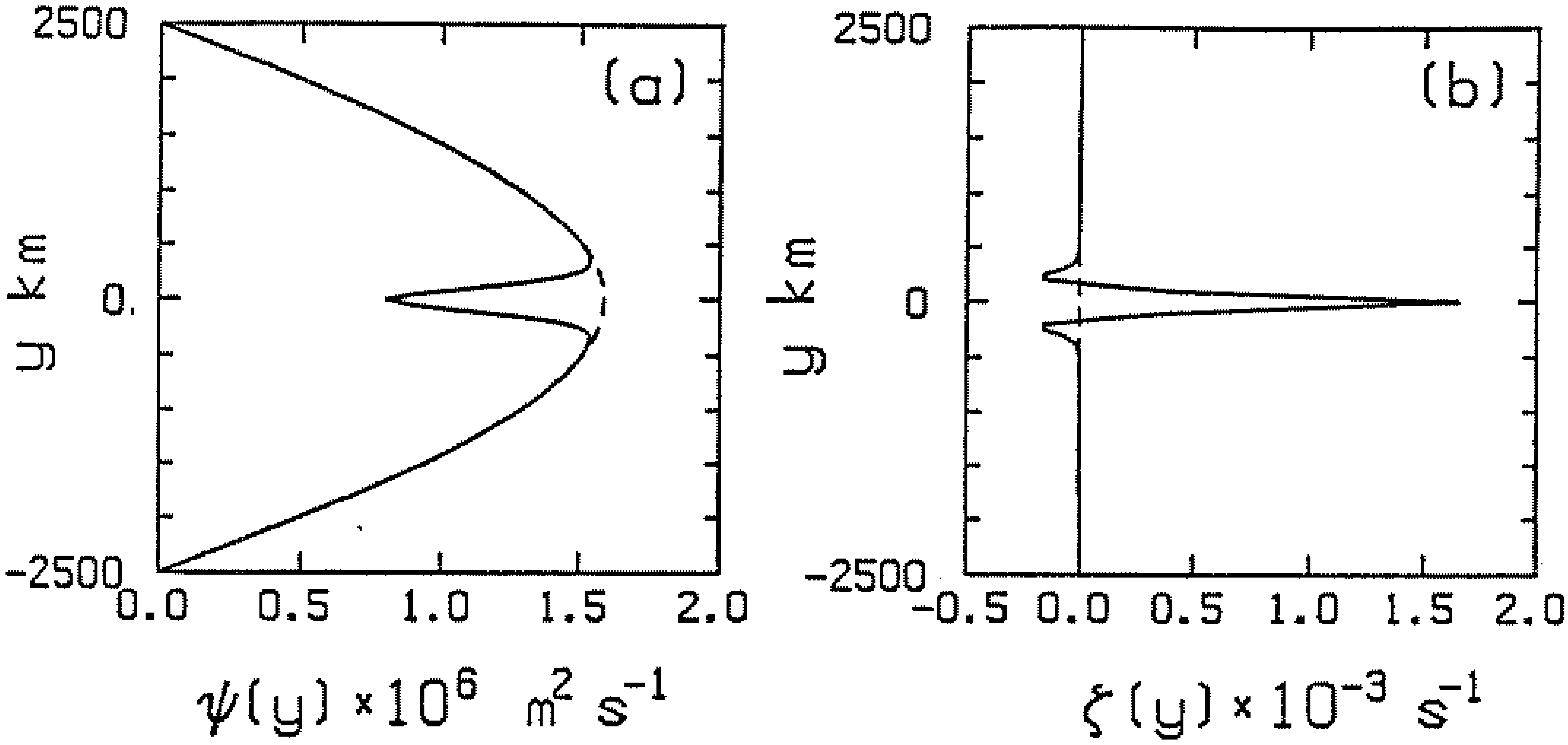

Figure 1. Cross-sections of (a) the total stream-function field and (b) the total vorticity field in the y direction at the initial time. Shown also are cross-sections of the environmental stream function and vorticity (dashed lines).

Eq. (2.2) is much larger everywhere in the domain than its environmental counterpart. A reason for choosing a relatively narrow profile is that it provides a severe test of algorithms to determine the vorticity centre (see section 3(b)), even at such a high horizontal resolution as 20 km. It can be expected that broader profiles allow a better reconstruction of the symmetric vortex, even with a coarser grid. However, the reconstruction becomes more difficult if the data available for the analysis have an irregular spatial distribution as is normal in the atmosphere. For this reason the experiments to be described represent a best-case situation for analysis.

With the foregoing initial conditions, the model was integrated in time for a period of 96 hours. At 48 hours the total stream-function and vorticity fields were stored on the 20 km × 20 km computational grid, and form the basis for a 'perfect' analysis at that time. Henceforth we refer to 48 hours as the 'analysis time'. The total stream function in the vicinity of the vortex at the analysis time is shown in Fig. 2(a). The asymmetric field can be obtained from this in two ways, either by subtracting both the imposed initial

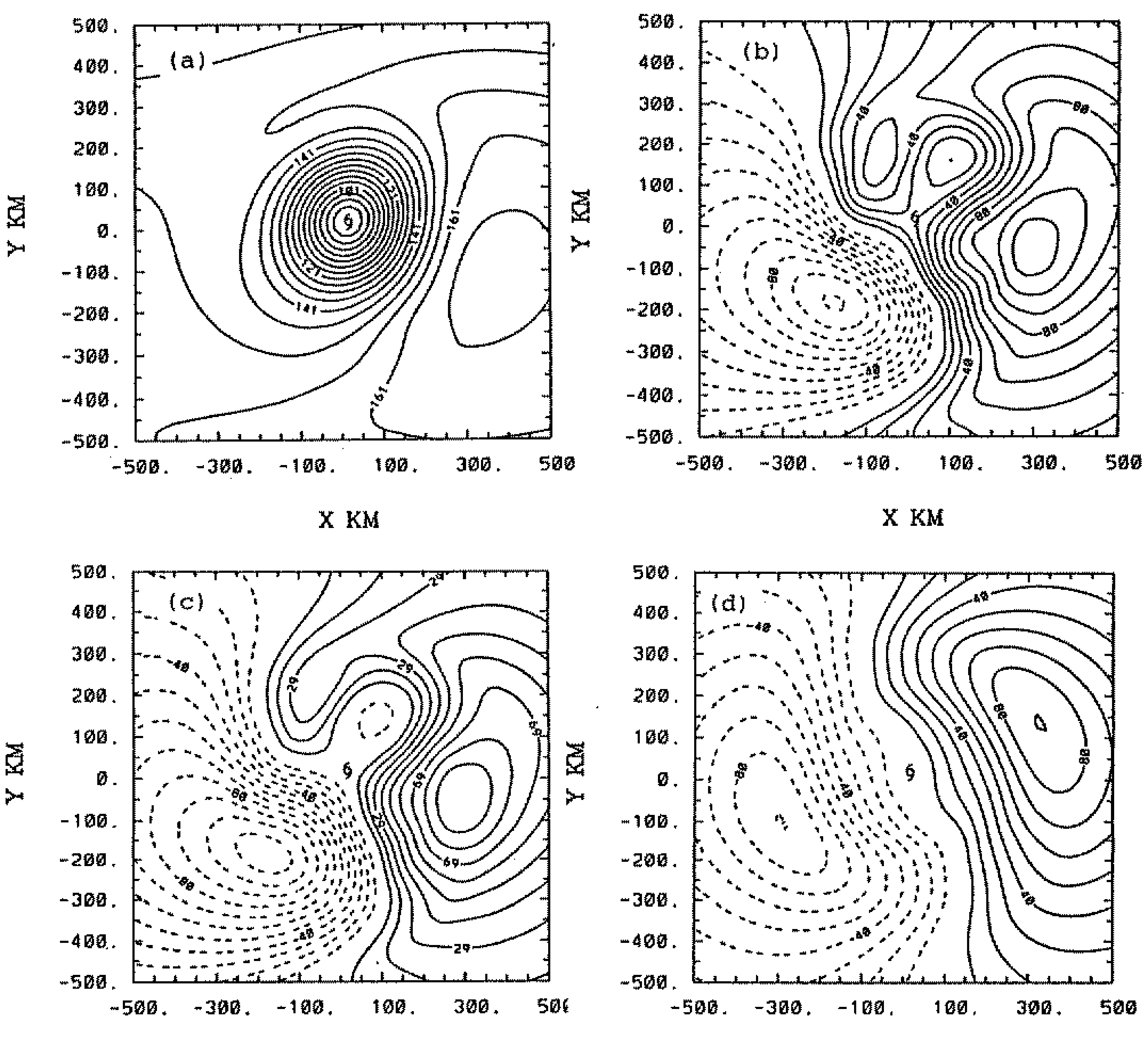

Figure 2. Vortex structure after 48 hours of model integration, i.e. at the analysis time: (a) total, (b) asymmetric stream function with the initial vortex removed, (c) asymmetric stream function with the symmetric vortex at the analysis time removed, and (d) azimuthal wave-number-one component of the stream function. Only a subdomain of the total computational domain is shown. Contour interval is $5 \times 10^5 \mathrm{~m}^2 \mathrm{~s}^{-1}$ in (a) and $10^5 \mathrm{~m}^2 \mathrm{~s}^{-1}$ in the other panels. The hurricane symbol denotes the vortex centre.

environment and the initial symmetric vortex from the total stream function, a method of partitioning suggested by Kasahara and Platzman (1963, their Method III), or by removing the environment and the symmetric field at the analysis time from the total stream-function field. The asymmetric fields resulting from these two methods, using the full 20 km × 20 km data set are shown in Figs. 2(b) and 2(c) respectively. They differ by a symmetric field that develops in time as the flow evolves (see, for example, Ross and Kurihara 1992).

Figure 2(d) shows the azimuthal wave-number-one contribution to the asymmetric part of the stream function which is of consequence for the vortex motion (see, for example, Smith 1993). The total stream-function and vorticity fields, possibly in a degraded form, are considered as an initial data set for a subsequent analysis and track forecast. When the resolution of the degraded data set was low (160 and 320 km resolution, described later), the analysis was carried out for the stream function only, because the relatively small-scale structure of the vorticity field was barely resolved in the vicinity of the vortex.

(*b*) *The degraded data sets*

The degraded data sets at the analysis time were extracted from the simulated data on regular grids with grid sizes of 40, 80, 160 and 320 km, in both the x and y direction. This may be accomplished in a number of ways. For example, at 40 km resolution one can divide the original data set into four submatrices, depending on which of the four grid points in the south-west corner of the original data set is chosen for the corresponding corner of the 40 km resolution grid. Thus, none of these submatrices contain the same data points and, in most cases for horizontal resolutions lower than 80 km, they differ substantially from each other in the vicinity of the vortex. In the subsets with moderate and low resolution, the symmetric vortex and the asymmetries are sometimes reasonably well resolved and sometimes hardly present. Thus to some extent each individual data subset can be regarded as a result of an integration of the numerical model starting from different initial conditions. At 80 km resolution, 16 submatrices can be formed and so on. Only subsets of possible submatrices at this and lower resolutions were examined. The degraded data sets were re-interpolated to the original 20 km grid with a birational spline scheme. The latter is similar to algorithms using bicubic splines, but employs simple rational functions instead of cubic polynomials for the interpolation (a brief introduction of the theory of rational splines is given by Press *et al.* (1986, 83ff); Späth (1991, 126ff) gives a detailed derivation). The advantage of this scheme, in comparison, for example, with schemes using interpolating bicubic splines or approximating Bezier-splines, is that the interpolated values are nearly bilinearly related to the original data between the coarse-grid-point locations, and that the curvature of the two-dimensional surface obtained by this procedure is a maximum at the original grid points used for the analysis. Mainly for the first reason, birational splines are preferable to an interpolation with bicubic splines, at least for the examples presented in this study, because they damp small-amplitude wave-like structures that otherwise would contaminate the subsequent analysis and its interpretation. The advantage of birational interpolation schemes in comparison with approximating schemes such as Bezier-splines is that the former preserve all functional values at the actual data points.

3. Data partitioning

At each grid point (i, j) in the domain, any field f_{ij} to be analysed can be decomposed into an environmental contribution f_{ij}^{E} and a vortex contribution f_{ij}^{V}, i.e.,

$$f_{ij} = f_{ij}^{\mathrm{E}} + f_{ij}^{\mathrm{V}}. \tag{3.1}$$

Further, the vortex field can be sub-partitioned into

$$f_{ij}^{\mathrm{V}} = f_{ij}^{\mathrm{VS}} + f_{ij}^{\mathrm{VA}} \tag{3.2}$$

where f_{ij}^{VS} denotes the symmetric vortex and

$$f_{ij}^{\mathrm{VA}} = \sum_{k=k_0}^{N} f_{ij}^{\mathrm{VA}k}$$

the sum of all asymmetric wave-number components up to azimuthal wave number N. If Kasahara and Platzmann's (1963) Method III is applied, f_{ij}^{VS} is independent of time and $k_0 = 0$, while in general f_{ij}^{VS} is time-dependent and $k_0 = 1$. The environmental flow can be sub-partitioned into

$$f_{ij}^{\mathrm{E}} = f_{ij}^{\mathrm{ES}} + f_{ij}^{\mathrm{EL}} \tag{3.3}$$

where f_{ij}^{EL} denotes the large-scale environment, defined to be only varying slowly on the scale of the vortex, and f_{ij}^{ES} consists of features belonging to the environmental flow that are of small horizontal scale compared with those of f_{ij}^{EL}. The field f_{ij}^{ES} must be considered in an analysis of real data, but it can be neglected in the present calculations because the environmental flow undergoes only small changes over the full integration period of 96 hours (these changes are associated *inter alia* with the generation of domain-sized Rossby waves by the vortex (see, for example, Smith *et al.* 1995)).

(*a*) *Extraction of the vortex environment*

The method to isolate the large-scale vortex environment f_{ij}^{EL} combines an iterative process, described by Barnes (1964), with a low-pass filter provided by a one-dimensional fast Fourier transform (Press *et al.* 1986, 495ff). In the first iteration step, the original field is smoothed out to produce a first guess f_{ij1}^{EL} for the environmental flow. This guess is subtracted from the original field to give the first difference field f_{ij1}^{D}. A new guess field f_{ijn}^{EL} ($n = 2, 3, \ldots$) can be obtained by smoothing f_{ij1}^{D} in the same way as before and setting

$$f_{ijn}^{\mathrm{EL}} = f_{ijn-1}^{\mathrm{EL}} + f_{ijn-1}^{\mathrm{D}} \tag{3.4}$$

which is used in turn for the next iteration step until convergence is achieved, i.e. until the difference between f_{ijn}^{EL} and f_{ijn-1}^{EL} is sufficiently small. In each iteration step, the one-dimensional low-pass filter is applied to smooth each individual column of f_{ij} (i.e. the functional values in the y direction). After this the filter is used to smooth each row (i.e. the x direction) of the matrix resulting from the first smoothing operation. During each step of the alternating column- and row-wise low-pass filtering, the linear trend is separated from the functional values of each row and column and the functional values are ordered into a vector of four times the original length of each row and column to make each signal in the x or y direction periodic and avoid problems with the one-dimensional Fourier analysis during the filtering. The second and fourth quarter of this vector contains the original functional values of each row or column, and the first and third quarter the negative of the original functional values. In addition, the functional values of each quarter of the vector are ordered antisymmetrically (mirror image) in space with respect to the values of the adjoining quarters. The Fourier analysis used by the low-pass filter is truncated at a certain wavelength which in the cases discussed here lies between 2500 and 4000 km. This ensures that the resulting large-scale component of the environmental flow is smooth on the scale of the vortex. Possible smaller-scale environmental structures (f_{ij}^{ES}) project onto higher wave numbers of the subsequent azimuthal Fourier analysis described in section 3(c). Application of the technique to isolate f_{ij}^{EL} gives acceptable results at all resolutions studied in our experiments as will be shown in section 5. Tests with real data are being carried out and will be the subject of a subsequent paper.

(*b*) *Location of the vortex centre*

In order to carry out an azimuthal analysis of the vortex structure, and indeed for the application of many analysis procedures, it is necessary to determine the vortex centre accurately, which, following Smith *et al.* (1990), we define as the location of the relative vorticity maximum*. A mislocation of the vortex centre, followed by an azimuthal analysis of a given vortical field, results in both an error in the extraction of the symmetric vortex and its asymmetries, and the spurious appearance of the neutral nonrotating mode of azimuthal wave-number one as discussed by Gent and McWilliams (1986) and Weber and Smith (1993). As shown later, the ubiquity of this mode can be exploited to design an accurate method for locating the vortex centre. It must be emphasized that the vortex centre can be adequately located only if the vortex is sufficiently well resolved by the data; if not, all centre-finding algorithms must fail. For a given vortical field on a rectangular grid, the procedure first locates the grid point where the vorticity is a maximum. Then a second-order polynomial is fitted through this grid point and the four points closest to it† to obtain a first guess for the vortex-centre position. Finally, a sequence of fields (at present 100), identical with the original field, but centred a small distance (typically 3–5 km) away from the first-guess centre, is computed from the original data field by birational interpolation. If these fields are subtracted from the original field, each resulting field contains the neutral nonrotating wave-number-one mode, but orientated differently. The extrema of this mode are located using an interpolating polynomial as before, and a straight line connecting these extrema defines the orientation of the mode. All intersections of these straight lines are calculated and then averaged to give a mean centre. In an iterative procedure, all intersections are eliminated from the ensemble that deviate by more than twice the standard deviation from the mean centre. Then the above procedure is repeated with the degraded ensemble until two consecutively computed mean-centre values differ only by a few metres, i.e. until the exact centre position is approximated successfully.

This method is superior to methods that use interpolating polynomials only, but its accuracy decreases with the grid resolution also, although not as fast as that of the foregoing methods. As noted above, if the symmetric vortex is not well resolved, or not at all resolved in the data field, an accurate determination of the 'true' vortex centre is not possible in general and it is necessary to obtain the centre position by different means, as in the experiments at 160 and 320 km resolution described later. However, the scheme for the location of the vortex centre is useful where the resolution of the data is adequate, but the vortex is situated in the wrong location. This may happen, for example, when a radar or satellite fix shows the cyclone centre to be displaced from the circulation centre in a first guess for the analysis which is provided by an earlier model forecast. On such occasions, the vortex must be removed from the data field before an initialization of the prediction model with a relocated synthetic vortex can proceed.

* Note that in discrete data fields, the vortex centre does not usually coincide with the location of a grid point, but lies somewhere between four surrounding points.

† Normally this simpler procedure is the one used to locate the vortex centre as, for example, in the barotropic numerical model of Ulrich and Smith (1991).

At 40 and 80 km resolution, the method described above gives an accurate estimate of the known vortex centre, and the subsequent analyses are carried out with this analysed centre. In contrast, at 160 and 320 km resolution the vortex is not well resolved, or even not at all resolved in the data fields, and the method is inapplicable. For these initial fields we carry out the azimuthal analysis about the known vortex centre, i.e. the vortex centre determined at 20 km resolution. This is necessary to be able to compare the components of the analysed field with those of the control calculation. However, it means that the results of the analysis must be regarded as providing an upper limit to the information that can be extracted from the degraded data set in question.

(*c*) *Extraction of the symmetric vortex*

When the environmental flow has been removed from the analysed field and the vortex centre has been located, the symmetric part of the vortex may be obtained. The method of determining the 'symmetric vortex' depends on the resolution of the available data for a given vortex size. The decomposition of the residual field into its symmetric and asymmetric components is achieved by a one-dimensional fast Fourier analysis in the azimuthal direction about the vortex centre, using birational splines for the interpolation of the data from the rectangular grid to polar coordinates centred on the vortex. This analysis method gives acceptable results near the centre of the vortex only if the data points there are relatively dense, or if the vortex centre happens to be close to a grid point. At lower resolutions ($\geqslant$100 km), or if the vortex centre is remote from a grid point, the magnitudes of symmetric stream function and vorticity at the vortex centre are generally underestimated, the error being dependent on the distance of the vortex centre from the nearest grid point.

(*d*) *The vortex asymmetries*

In the flow partition described here, the residual field that remains when both the vortex environment and the symmetric vortex have been removed from the analysed field constitutes the vortex asymmetries. Specifically, this field is the sum of azimuthal wave-number components greater than zero obtained by the Fourier analysis, truncated at a wave number that can be tolerably resolved with the particular distribution of data points relative to the vortex centre. In the analyses at 40 and 80 km, the truncation wave number used for the re-initialization of the numerical model is four, in those at 160 km it is two, and in those at 320 km it is one. However, in the asymmetric fields shown in the figures of section 5, the truncation wave-number six is chosen to facilitate comparison with the components of the analysed fields and their original counterparts. The wave-number-one component may contain remnants of the neutral nonrotating wave-number-one mode (see section 3(b)) which can be removed by selectively smoothing this field.

Since current practice normally requires that the analysis of a tropical cyclone be carried out with data at a horizontal resolution lower than 200 km, there would be little merit in determining the azimuthal wave-number components higher than one because of aliasing effects caused by interpolation before the azimuthal Fourier analysis. Even an approximate determination of the wave-number-one component, or, indeed, the symmetric vortex itself, may be very difficult for the same reason. Moreover, in contrast to the model fields created here, it can be expected that the environment as defined in sub-section 3(a) is not smooth in the immediate neighbourhood of the cyclone, and that the data fields used for the analysis contain irregular features that are of relatively small horizontal scale (i.e. the contribution f_{ij}^{ES} in the expression (3.3) must be taken into account). The partitioning implied by our analysis technique is such that these features project onto the higher wave numbers in the azimuthal Fourier analysis. Therefore, it would seem appropriate in general to regard all azimuthal wave-number components higher than one as part of the environmental field and to *define* 'the vortex asymmetry' as the wave-number-one component of the azimuthal Fourier analysis. It is only this component that is of consequence for the vortex motion. Note that, in this decomposition, the flow at the vortex centre associated with the 'small-scale' environmental contribution is zero by definition; the non-zero contribution from f_{ij}^{ES} is contained in the vortex asymmetries. With this partition in mind we use the term 'vortex asymmetries' to mean the azimuthal wave-number-one component and higher.

4. Symmetric vortex enhancement

In the analyses at 40 and 80 km resolution discussed in the next section, the analysed symmetric-vortex profile differs relatively little from that of the original symmetric vortex at the analysis time and can be used for the subsequent re-initialization. However, in the analysis at 160 km resolution this is not so and we proceed as follows. If the nearest grid point is located beyond a certain distance from the vortex centre, typically 40 km, the magnitude of the symmetric stream function at the vortex centre is obtained by linearly extrapolating from the point located at the steepest part of the symmetric profile determined by the Fourier analysis. Together with two other values taken from this profile at larger radii, the extrapolated centre value is used to define a synthetic vortex by fitting the profile given by Eq. (2.2) to these points. The assumption is that, far from the vortex centre, the analysed symmetric field is an adequate representation of the true field. The choice of the profile is arbitrary and other profiles may prove to be just as good or better. However, one would expect the precise shape of the symmetric profile to have only a minor direct impact on the subsequent vortex track, unless the synthetic vortex itself is used to generate the vortex asymmetries, e.g. by an application of the truncated-wave-number model of Ross and Kurihara (1992) or the extended analytic theory of Smith and Weber (1993). The symmetric field obtained from the azimuthal Fourier analysis is now replaced by the synthetic vortex. When applied to the stream-function fields of the analyses carried out at 160 km horizontal resolution in section 5(d), this method is more satisfactory than using the analysed symmetric vortex itself. Note that the assumption that the vortex centre is known is the only additional information required in this case for the analysis to proceed.

At 320 km horizontal resolution, the foregoing method is not applicable either and is replaced by one in which the maximum tangential wind speed, its distance from the vortex centre, and the radius of gale-force wind ($15\,\mathrm{m\,s^{-1}}$) is specified. First, a new approximation to the stream-function-centre amplitude is determined by fitting an analytic profile to these additional data. Afterwards, the symmetric vortex is generated in the manner described earlier for 160 km resolution. Several analytic one- and two-parameter profiles were tested to estimate the known centre amplitude, including the one used by Chan and Williams (1987, $b = 1$). None of these yielded acceptable results in recovering the known stream-function-centre amplitude, the typical errors being more than 30%, depending on the case investigated. Profiles with more than two parameters, which require additional information about the kinematic structure of the symmetric vortex, have not been investigated yet.

The method described above for the construction of a synthetic vortex does not lay claim to being general and is most likely capable of improvement. Normally, in practice, the data sets available for an analysis have a resolution below 200 km. For example, the data used for the initialization of TAPS are provided on a grid with approximately 250 km horizontal resolution (K. Puri, personal communication). In this case, especially if the vortex is barely resolved in the data, additional data (possibly synthetic) are required to construct the symmetric vortex, such as the estimated minimum central pressure, maximum tangential wind speed, and the radius of the outermost closed isobar, instead of that provided by an azimuthal analysis. Apart from the fact that the accuracy of the additional data is usually uncertain, except possibly where obtained from aircraft reconnaissance, the question is to what extent the symmetric vortex resulting from the azimuthal analysis can be used for a better representation of the structure of a particular tropical cyclone. It is hoped that possible answers to this question, and the generalization of the methods described above, will be discussed in a subsequent paper.

5. Results

We describe now the results of the series of analyses in which the resolution of the data at the analysis time is progressively degraded. It should be borne in mind that the results are dependent on the size of vortex chosen, so that broader vortices will be better resolved by a given resolution (Reeder *et al.* 1992).

On completion of each analysis, the vortex environment, symmetric vortex and vortex asymmetries are summed and used to re-initialize the numerical model. The model is then integrated for another 48 hours and the resulting vortex track compared with that in the control run. These experiments enable one to determine the adequacy of the analysed fields at different resolutions for the purpose of predicting the subsequent vortex track. At lower resolutions (160 and 320 km), the analysed vorticity field is unsatisfactory for re-starting the numerical integration, because the relatively small-scale structures of the actual field are not resolved in the analysis. Instead the vorticity field is calculated from the stream-function distribution at the analysis time, using the relationship $\zeta = \nabla^2\psi$ in finite-difference form with a 20 km horizontal grid size. At these resolutions we calculate also the tracks resulting from an initialization of the numerical model with the vortex asymmetries excluded to determine the direct impact of these asymmetries on the vortex track. Furthermore, we include the tracks of the symmetric vortex resulting from the analysis alone for comparison with the tracks produced by the synthetic vortices. However, in some analyses at 320 km resolution the analysed symmetric vortex is hardly recognizable as being a vortex at all and, therefore, the subsequent tracks are not very meaningful.

(*a*) *Analysis of the original data field*

First we apply the analysis to the complete data set provided by the numerical model integration at 48 hours to investigate the extent to which the individual components of the field can be restored. The vorticity and stream-function fields obtained by the method to extract the environmental component from the total field described in section 3(a) are not shown because they are almost identical to the initial environmental fields shown in Fig. 1. The environmental stream-function field can be reconstructed to within a maximum relative error of about 1%, and the maximum relative error of the environmental vorticity is below 4%. The latter result is perhaps surprising because the magnitude of the environmental vorticity is much smaller in the whole domain than the magnitude of the symmetric vorticity field.

The situation is different for the symmetric fields. The relative difference between the initial symmetric stream function and the symmetric profile resulting from the analysis at 20 km resolution is large outside the core region, while the difference is relatively small (5%) within. The initial symmetric stream function is negative throughout the whole domain and very small at large distances from the vortex centre. The analysed symmetric stream function is positive from a radius of about 340 km outwards to 1700 km and has a local maximum at 500 km radius with a magnitude of approximately 100 times that of the initial symmetric stream function at the same distance from the centre. It decays with growing radius, but not as fast as the initial stream function. The main reason for the discrepancy is that the symmetric circulation evolves as the vortex moves on the beta-plane (see, for example, Smith *et al.* 1995); therefore, its structure at 48 hours is not equal to the initial vortex structure. The time-dependent symmetric field, which in the Kasahara–Platzman Method III of partitioning is regarded as a part of the vortex asymmetries, has a relatively small magnitude near the centre of the vortex, but at large radii it decays more slowly with radius than the initial profile. Accordingly, its magnitude is larger than that of the initial profile in the outer part of the domain. However, there is no way to determine the initial symmetric vortex at the analysis time. Indeed, in the spirit of the present experiments, the 'initial' configuration should not be assumed to be known. The evolution of the symmetric component of flow from the initial time influences the vortex track through feedback into the wave-number-one component and may need to be taken into account in the construction of a synthetic vortex including the asymmetries (Ross and Kurihara 1992).

The analysed fields at this resolution are shown in Fig. 2 and have been discussed in section 2(a). Note that the analysed asymmetries have some small-scale structures which are associated with higher azimuthal wave-number components induced by the vortex and by the environmental flow (Fig. 2(c)).

(*b*) *Analysis at* 40 *km horizontal resolution*

In the second experiment the simulated data fields at 48 hours are split up into four submatrices of 40 km horizontal resolution as explained in section 2(b). These four fields are analysed separately. The results of one of the analyses are displayed in Fig. 3 and compare well with the analysis at 20 km resolution shown in Fig. 2. The differences between the total asymmetric field (including the wave-number-zero component) in Fig. 3(b), and that in Fig. 2(c) are small, the relative errors being smaller than 1%. The analysis errors in restoring the environmental component and the initial symmetric vortex are of the same order of magnitude as in the last sub-section.

One feature worth noting already is the relative smoothness of the wave-number-one contribution (Fig. 3(c)) compared with the original field (Fig. 2(d)). The same is true for the analysed vorticity field (not shown). The inherent smoothing of the analysis method reduces the magnitude of the gyre structures, although the dominant features are correctly represented to within a few per cent. The other three cases analysed at this resolution give essentially the same results as the one presented in Fig. 3, with comparable errors.

The numerical model was re-initialized with the four new analyses (azimuthal wave-number components less than or equal to four) in turn and integrated for a further 48 hours. Comparison of the tracks so obtained with that of the control run gives centre-position errors not exceeding 20 km at the end of the calculations, i.e. the errors are within the horizontal resolution of the numerical model.

(*c*) *Analysis at* 80 *km horizontal resolution*

When the original fields are split up into a set of submatrices, each with a horizontal resolution of 80 km, the analysis delivers fields such as those shown in Fig. 4. The structure of the original fields in Fig. 2 is still captured quite well, but there is some loss of detail as can be seen by comparing for example the wave-number-one contribution of Fig. 4(c) with those in Figs. 2(d) and 3(c). An error analysis shows that the original total

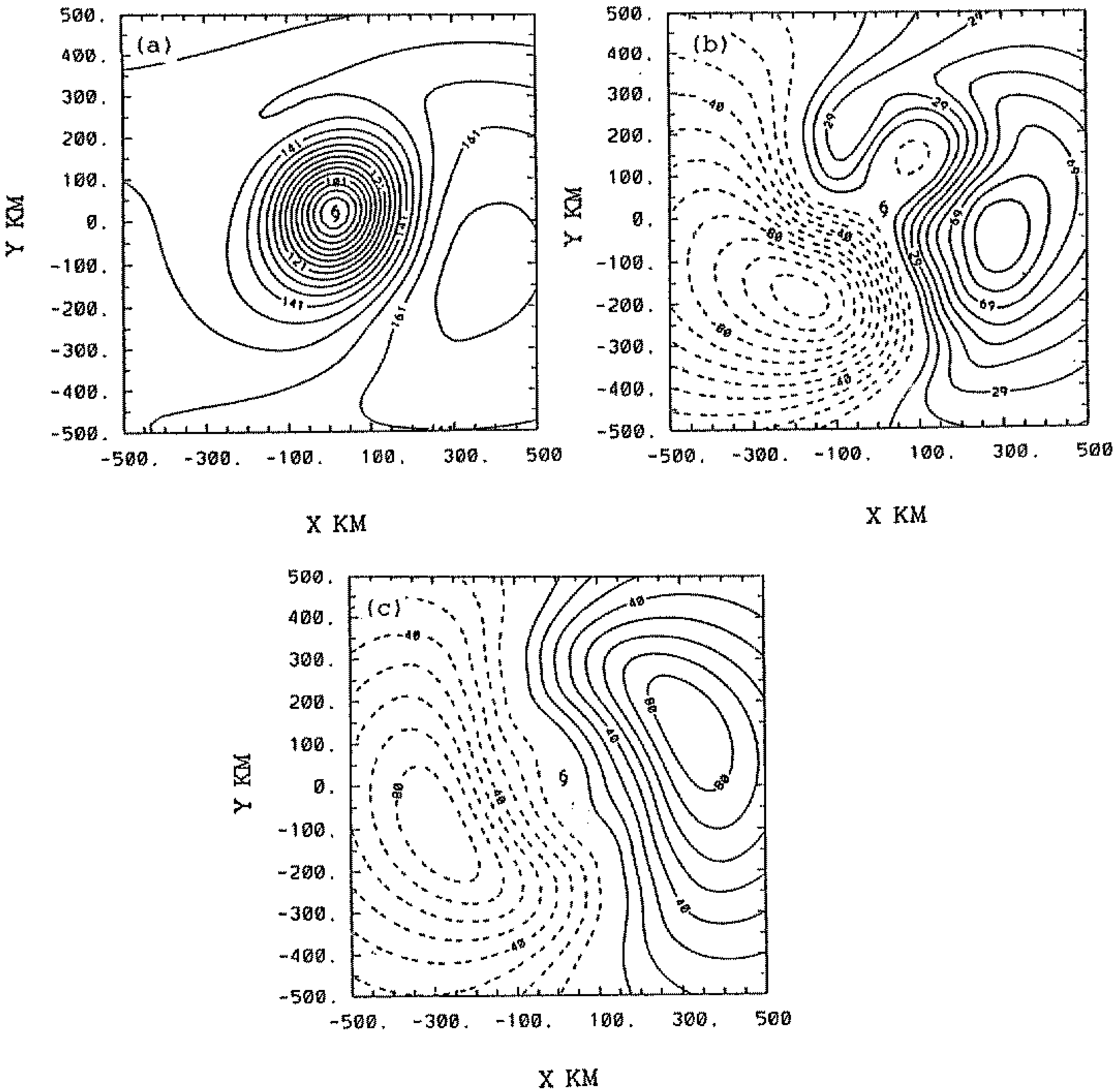

Figure 3. (a), (b) and (c) as in Figs. 2(a), (c) and (d), respectively, but for an analysis with 40 km horizontal resolution.

stream function is better represented (maximum error 5% at the vortex centre) than the vorticity (up to 20% relative error at the vortex centre). In all six cases investigated, the centre amplitudes of the stream function are underestimated to a degree that depends on the distance of the vortex centre from the nearest grid point. The error of the analysed symmetric stream function is generally small; it is largest near the vortex centre with a maximum relative deviation of about 2.5% from the true symmetric stream function at analysis time. Therefore, the analysed symmetric fields are not modified and can be used directly for the re-initialization of the barotropic model. The environment is restored with a maximum relative error of only about 1% in the whole domain as before. Reconstruction of the asymmetric stream-function field, truncated at wave-number four, shows small errors below $2 \times 10^4\,\mathrm{m^2s^{-1}}$ (cf. Fig. 2(c)) at radii greater than 100 km, whereas the errors are relatively large (of order $10^5\,\mathrm{m^2s^{-1}}$) near the vortex centre. Truncation at wave-number six yields approximately the same errors (Fig. 4(b)). In all probability these errors, which show a wavelike structure in the azimuthal direction, are

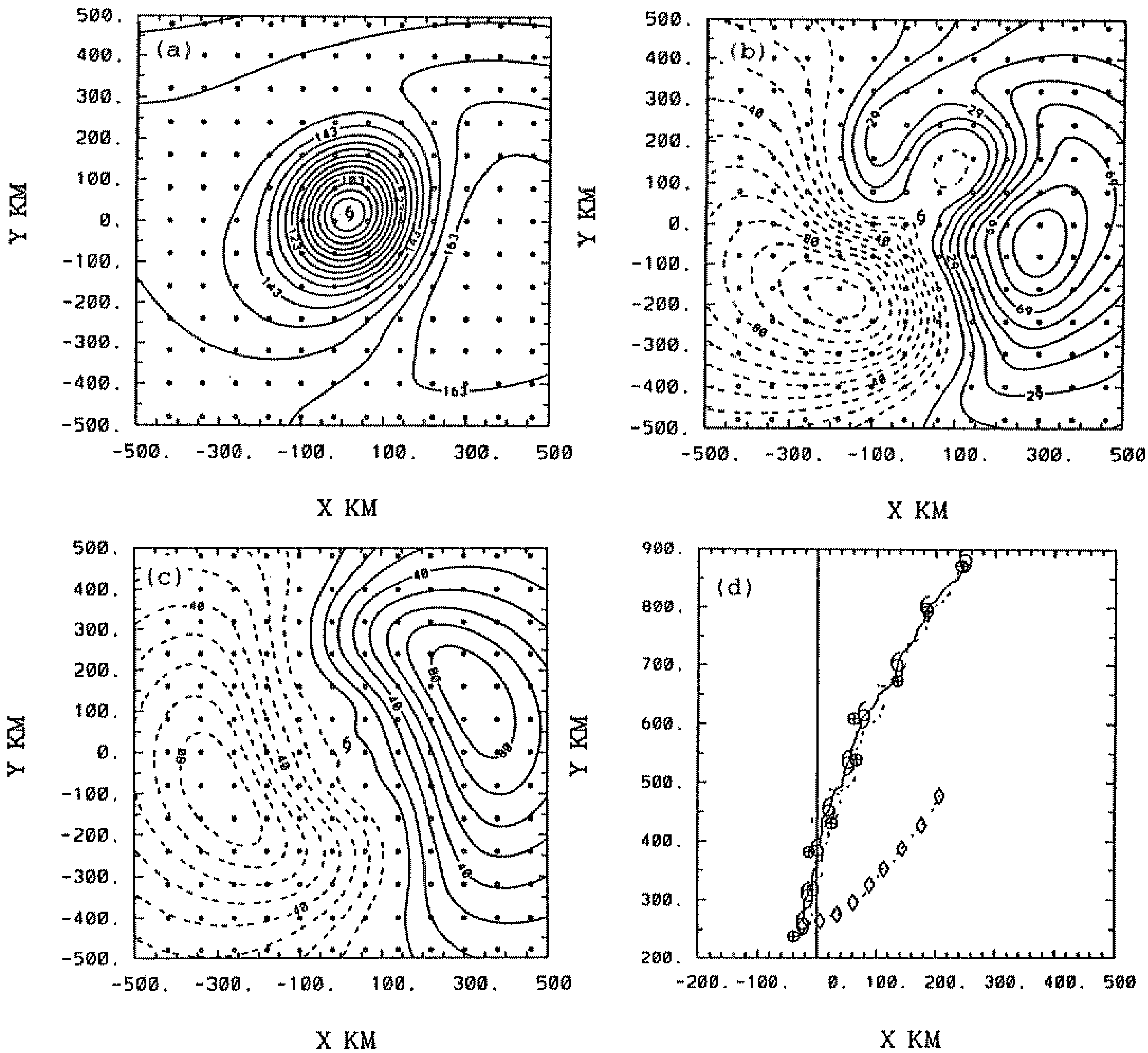

Figure 4. (a)–(c) correspond with Figs. 2(a), (c) and (d), but for an analysis with 80 km horizontal resolution. The small circles denote the grid-point locations used for the analysis. Panel (d) compares one vortex track for an integration started with the analysis (encircled cross symbols) with that in the control calculation (hurricane symbols) and that resulting from an initialization of the numerical model with the symmetric vortex without the vortex asymmetries (diamond symbols). The symbols in each case show the vortex-centre position at six-hourly intervals.

caused by the interpolation procedure. The wave-number-one component represents the true structure well, with errors below $5 \times 10^3\,m^2s^{-1}$ farther away ($\geqslant$100 km) from the vortex centre (cf. Figs. 4(c) and 2(d)), while near the centre there exists the neutral nonrotating mode caused by a mislocation of the vortex centre. The maximum magnitude of this mode is relatively small, i.e. generally below $10^5\,m^2s^{-1}$. The larger-scale wave-number-one gyres are oriented correctly and the calculated drift speed of the vortex agrees well with the true speed at the analysis time when the inner gyres are eliminated. The residual field remaining after the extraction of the symmetric part and all asymmetric contributions up to wave-number four is small, with a maximum magnitude of about $3 \times 10^5\,m^2s^{-1}$. Consequently, the loss of information by truncating the asymmetric field at wave-number four is negligibly small.

One example of the track calculated after re-initialization of the numerical model is shown in Fig. 4(d). In all our investigations the agreement with the control is satisfactory, the tracks being nearly identical up to 24 hours and deviating by a maximum of about 40 km after 48 hours integration time. In each case the correct direction is maintained over the whole 48-hour period. On one occasion the analysed vortex drifts faster than in the control run but at all other times drifts more slowly. Possible reasons for this behaviour may be structural differences in the symmetric profile used for the re-initialization or, in the latter examples, the smoother and rather damped structure of the wave-number-one contribution. For each investigation, the initial centre position is correctly located, the errors being much smaller than the grid resolution of the numerical model. The track resulting from an initialization of the numerical model with the analysed symmetric vortex and environmental flow only (without the asymmetries) is included for comparison. After 48 hours integration the deviation from the control track is approximately 400 km, showing that the vortex asymmetries, initialized in the numerical model at the analysis time, are responsible for a little over 50% of the northward drift of the vortex. Without the asymmetries, the symmetric vortex develops new beta-gyres and, therefore, drifts polewards more slowly than the complete vortex including the asymmetries.

It is noteworthy that the tracks have a more erratic movement if the birational spline interpolation scheme is replaced by a scheme using bicubic splines. In all probability the wobbles in the track are caused by smaller-scale, small-amplitude wave structures at locations between the data points induced by the bicubic splines. The application of birational splines reduces the magnitude of these features and thereby the wobbles in the tracks.

(*d*) *Analysis at* 160 *km horizontal resolution*

The next series of experiments uses six submatrices of 160 km resolution for the analysis and the re-initialization. Figure 5 shows a typical example of fields obtained by the analysis. The structure of the perfect-analysis fields is still preserved, but the features of these fields are broadened and smoothed out by the interpolation. The centre amplitudes of the symmetric stream function and vorticity obtained by the azimuthal Fourier analysis are considerably underestimated when compared with the initial profiles; the amounts range from 20 to 30% for the stream function and about 50% for the vorticity, again depending on the distance of the nearest grid point from the vortex centre. Accordingly, a synthetic vortex was generated using the method explained in section 4 to improve the vortex structure, especially in the core region. The analysed asymmetric stream function truncated at wave-number six still resembles the original structure (cf. Fig. 5(b) with Fig. 2(c)), but smaller-scale details have mostly vanished as can be seen also, for example, by comparing Fig. 5(c) with the original wave-number-one component of Fig. 2(d). Maximum errors in the total asymmetric stream function occur within a circle of 200 km about the vortex centre with magnitudes below $2.5 \times 10^5\,\mathrm{m^2s^{-1}}$. The magnitude of the error is approximately the same as that of the azimuthal analysis truncated at wave-number two which was used to re-initialize the numerical model. This indicates that wave-number components higher than two are relatively unimportant. It should be noted that the azimuthal analysis was carried out about the known vortex centre instead of the centre determined from the 160 km resolution analysis; therefore it represents the maximum possible information that can be obtained at this resolution. The residual field after the truncation of the azimuthal analysis has an absolute maximum of $3.6 \times 10^5\,\mathrm{m^2s^{-1}}$ (truncation at wave-number two) and $3.2 \times 10^5\,\mathrm{m^2s^{-1}}$ (truncation at wave-number six) near the vortex centre, which is approximately one third of the absolute maximum of the total asymmetric stream-function field. This shows that the magnitudes of wave-numbers three, four, five and six are relatively small compared with wave

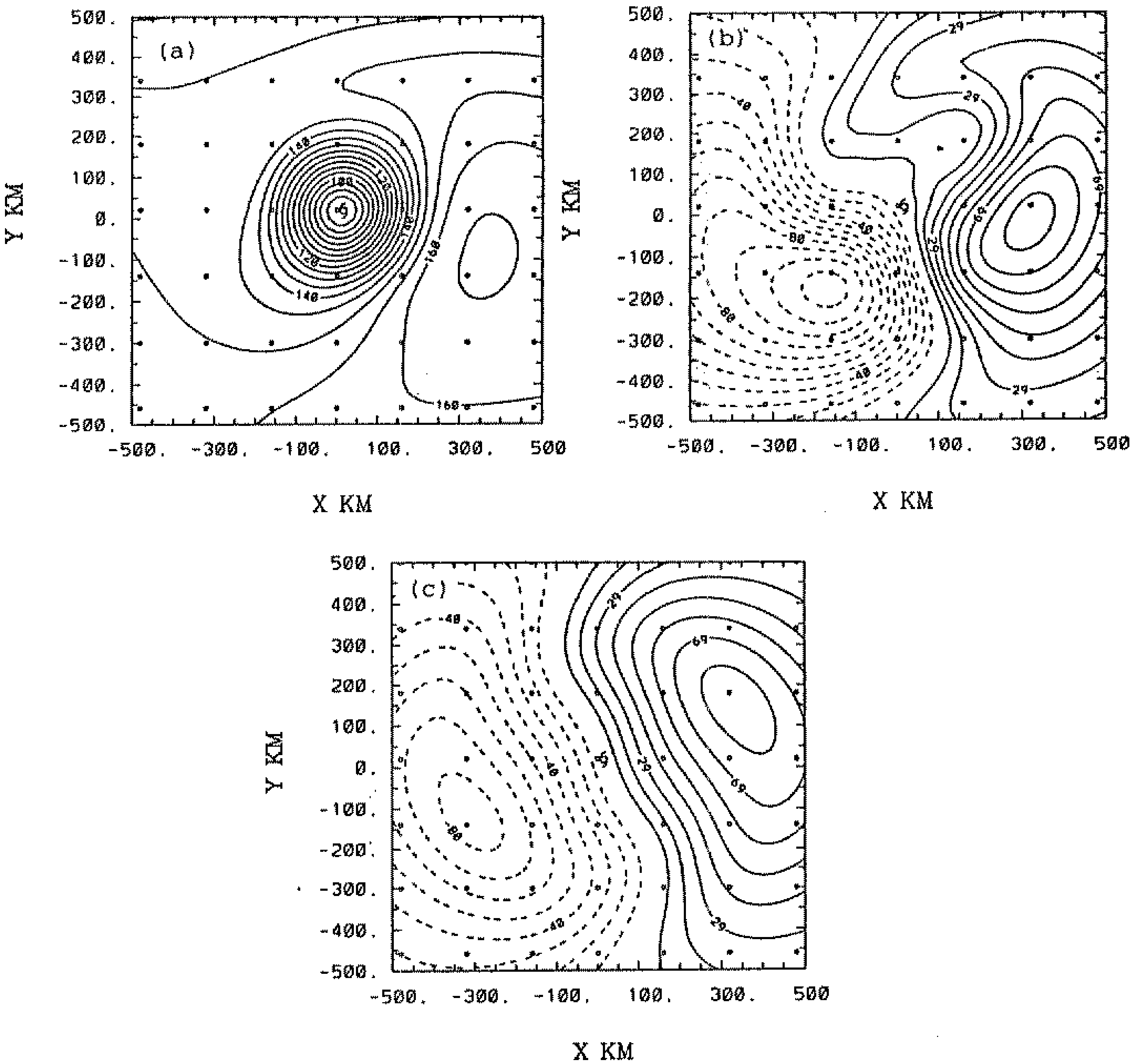

Figure 5. As in Fig. 2(a), (c) and (d), but for an analysis with 160 km horizontal resolution.

numbers one and two. The environmental field can still be reconstructed to within about 1% deviation from the original environment. At 160 km resolution, irrespective of how the grid points are located relative to the vortex centre, it is unnecessary to prescribe additional synthetic data to determine the symmetric-vortex profile adequately; indeed, at this resolution, each available data set itself contains sufficient information for a satisfactory reconstruction of the symmetric and asymmetric component of the narrow vortex, provided that the azimuthal analysis can be carried out about the correct vortex centre.

The resulting tracks of the six investigations are displayed in Fig. 6. Shown also are the tracks resulting from an initialization without the vortex asymmetries and those resulting from an initialization with the analysed symmetric vortex instead of the synthetic vortex, but including the analysed asymmetries. On three occasions (Figs. 6(c), 6(d) and 6(f)) the initial positions of the analysed vortex, located by fitting a second-order polynomial (cf. section 3(b), footnote), are inaccurate, deviating by up to 30 km from

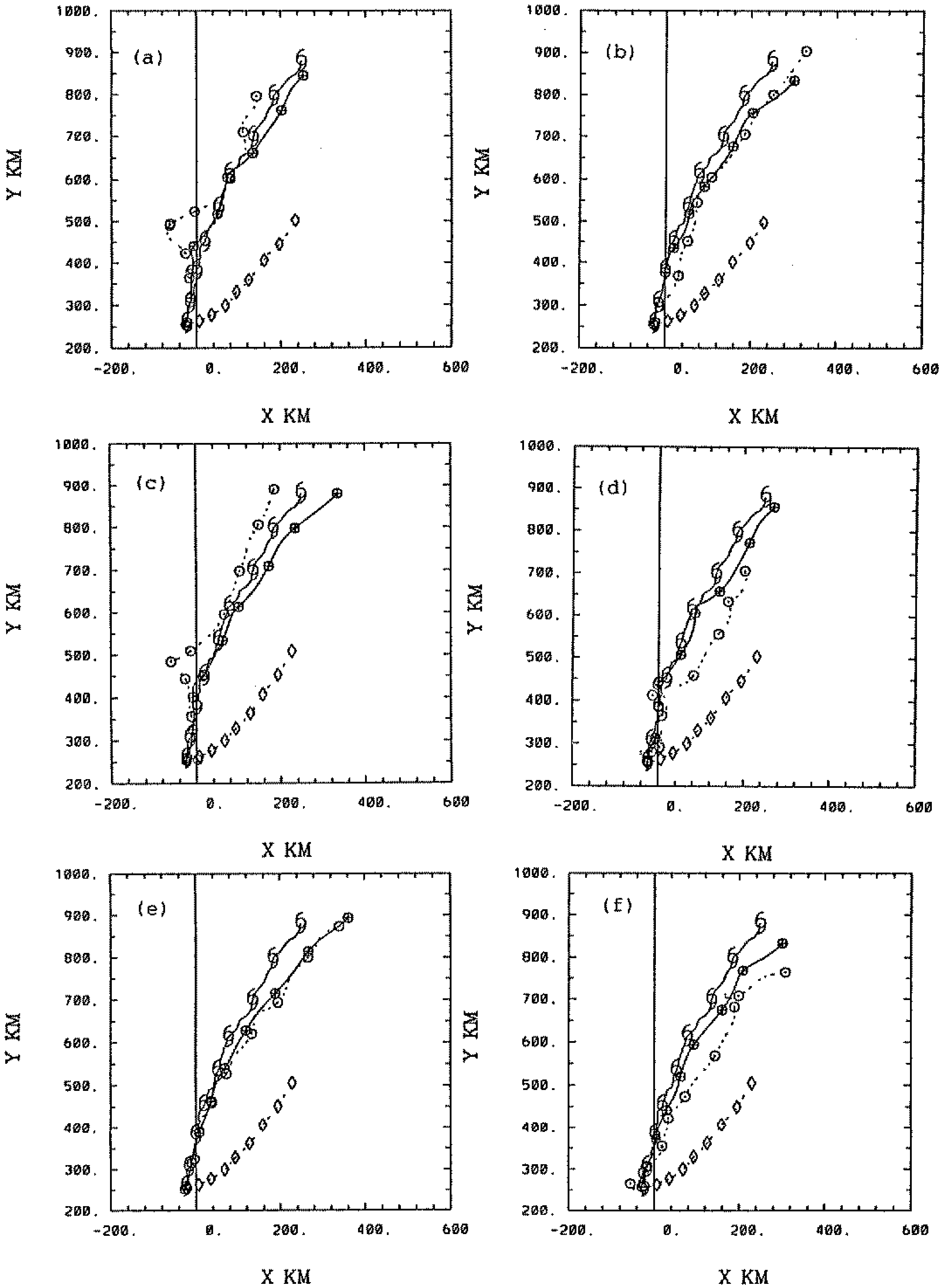

Figure 6. Vortex tracks based on the six sets of simulated initial data analysed at 160 km horizontal resolution. The symbols denote vortex-centre positions at six-hourly intervals as follows: the synthetic vortex including the vortex asymmetries (encircled cross symbols), the control run (hurricane symbols), analysed vortex including the vortex asymmetries (encircled dot symbols) and the synthetic vortex without the vortex asymmetries (diamond symbols).

the known position. The errors arise because the combination of a weak analysed symmetric vortex with the analysed asymmetries and the environmental flow during the re-initialization phase of the numerical model may yield a velocity distribution which is maximum at a location away from the centre of the weak symmetric vortex itself. After 24 hours the track forecasts using the synthetic vortex are always superior to forecasts without it, with, at worst, less than 40 km deviation from the control run (Fig. 6(d)). After 48 hours the tracks produced with the synthetic vortex (cf. section 4) are superior four times out of six (Figs. 6(a), 6(b), 6(d) and 6(f)), while in the other two the analysed vortex yields the better track. This indicates that a change of the symmetric profile alone may not lead to an improved track prognosis if adequate asymmetries are included in the re-initialized field. It should be noted, however, that the tracks computed with the analysed vortex tend to be erratic (especially in Figs. 6(a), 6(c) and 6(d)). A reason for this may lie in possible interactions of the weaker symmetric vortex with the comparably strong asymmetries or in successive mislocations of the vortex centre by the centre-finding algorithm for the same reason as mentioned above. The tracks of the synthetic vortex are steadier than those of the analysed vortex and maintain an approximately correct direction throughout the 48-hour integration time, with a maximum deviation of about 110 km (Fig. 6(e)), whereas the maximum deviation is 190 km for the analysed vortex (Fig. 6(d)). These results indicate that, for the vortex size used here, a horizontal resolution of 160 km is sufficient to provide reasonably accurate track forecasts without the need to use additional information for the generation of the symmetric-vortex profile. Although the interpolation procedure introduces errors into the analysis field, in all six experiments the analysis still captures the necessary features to achieve an acceptable prediction of the track. On the other hand, a forecast error of 110 km after 48 hours with a simple flow configuration such as the one used here suggests that 160 km resolution is a lower bound for an adequate track prediction of this particular vortex.

(*e*) *Analysis at* 320 *km horizontal resolution*

The analysis situation changes dramatically for the present vortex if the resolution of the initial data is reduced to 320 km. Except for the environmental component, which can be reconstructed still to within about 1% relative error in the whole domain, it is no longer possible to determine adequately the symmetric-vortex structure (relative errors up to 80%, corresponding with absolute errors of $6 \times 10^6\,m^2s^{-1}$ for the stream function) and the asymmetries (maximum absolute errors up to $6 \times 10^5\,m^2s^{-1}$ in a circle with a radius of 700 km measured from the vortex centre) from the given data distribution.

Figure 7(a) shows the analysed total stream-function field of one of the five studies, where the centre of the vortex was situated close to the centre of the square made up by four original grid points. In this experiment, without the use of any synthetic data, the symmetric vortex is barely captured by the analysis (the corresponding track is shown in Fig. 8(b), where the vortex-centre positions are denoted by encircled dots). In another experiment (not shown), where the vortex centre lies within 20 km radius of a grid point, the centre amplitude is determined reasonably well, but the radial extent of the symmetric vortex is considerably overestimated. For this reason it is necessary to prescribe additional information to define the symmetric vortex. As a first approach we specified a maximum tangential wind speed of $40\,m\,s^{-1}$ at a radius of 100 km and a radius of gale-force wind ($15\,m\,s^{-1}$) of 240 km, essentially the values of the initial vortex, and used an analytic vortex profile (e.g. the vortex used by Chan and Williams 1987) to estimate the centre amplitude of the stream function. Then, again, the profile given by Eq. (2.2) was fitted to this centre amplitude and to two additional values of the analysed symmetric field at larger radii. A problem here is the optimum choice of profile used to determine the

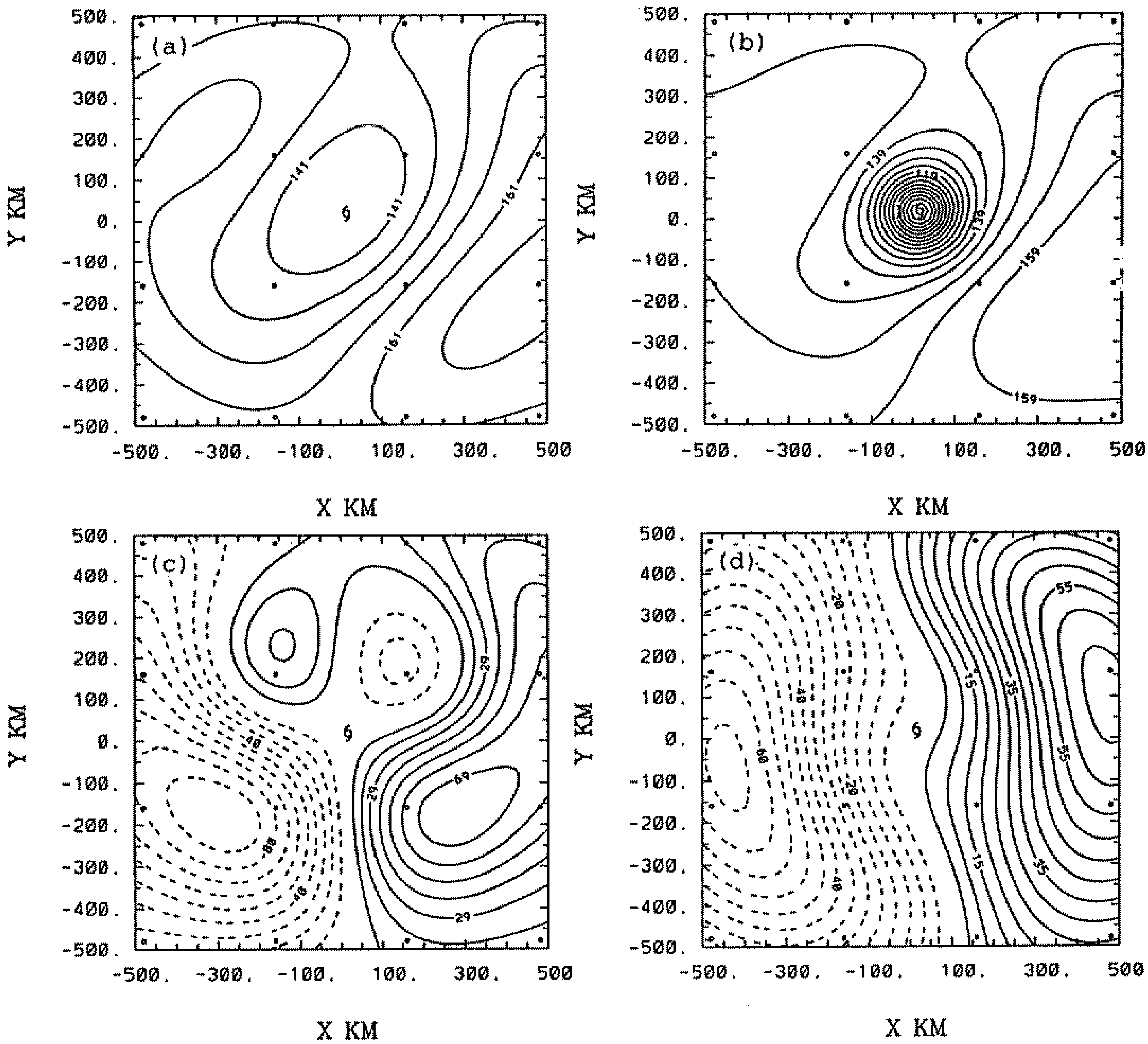

Figure 7. (a) Total asymmetric stream function obtained by an analysis at 320 km horizontal resolution in a case in which the vortex centre lies at the centre of a square made up by four grid points and in which no synthetic observations are used. It should be compared with Fig. 2(a). (b) Total stream function for an analysis at this resolution for an experiment where a synthetic vortex was added (see text for details); (c) and (d) show the asymmetric stream function and wave-number-one contribution thereof corresponding with panel (b). The hurricane symbol denotes the vortex centre.

centre amplitude. Various profiles were tested, but none of them was able to produce an adequate centre value corresponding with the known value of the stream function at the centre of the vortex. Another problem is the bias of the symmetric field caused by remnants of the asymmetric field, which is inevitable if interpolation schemes are applied to a sparse data set. If, as in the second step of the generation of the symmetric vortex, the profile (2.2) is fitted to data points at larger radii produced by the Fourier analysis, the result may be a vortex that is either much broader or much narrower than the original vortex. An example of the latter is displayed in Fig. 7(b), which should be compared with the original field in Fig. 2(a). Figures 7(c) and 7(d) show the total asymmetric stream-function field and the wave-number-one component for this example. The analysed asymmetries poorly represent the true structure (cf. Figs. 2(c) and 2(d)); the maximum amplitude of the wave-number-one component is underestimated by about 30% and,

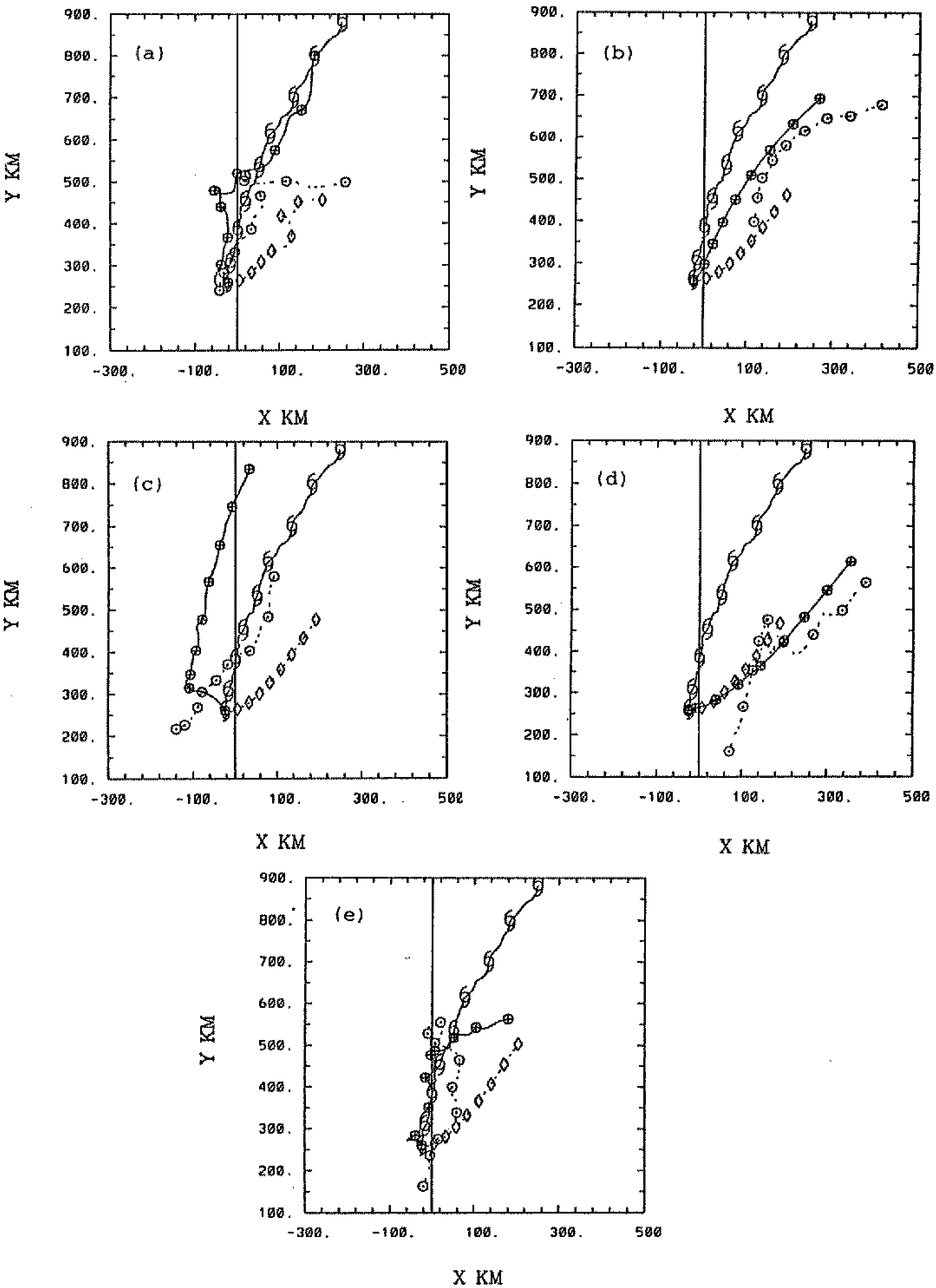

Figure 8. As in Fig. 6, but for an analysis with 320 km horizontal resolution.

more importantly, its orientation* is incorrect, presumably also as a result of aliasing effects caused by remnants of other wave numbers, including wave number zero, during the interpolation procedure. As a consequence, the vortex track is initially more eastward and later more southward when compared with that in the control run, with deviations of 85 km after 24 hours and 190 km after 48 hours as shown in Fig. 8(b). Some of the other studies at this resolution show an even greater error in the orientation of the wave-number-one asymmetry in comparison with the true structure; the maximum deviation of the track when compared with the track in the control run is 425 km after 48 hours.

The forecasts using the synthetic vortex with the analysed asymmetries are always superior to the forecasts with the analysed vortex and to the forecasts produced with the synthetic vortex without the asymmetries. The initial-position errors are large for the analysed vortex for the same reasons as mentioned in the last sub-section. In four experiments (Figs. 8(b), 8(c), 8(d) and 8(e)) the symmetric vortex resulting from the analysis is barely recognizable as a vortex and, therefore, the tracks are hardly meaningful. However, *none* of the tracks shown in this section adequately represents the control track. They indicate that neither the symmetric vortex (synthetic vortex *and* analysed symmetric vortex) nor the asymmetries can be recovered satisfactorily from the data sets. Both parts of these flow components have to be replaced by synthetic fields.

6. Summary and discussion

We have described a methodology for assessing analysis strategies for tropical cyclones for which the data base is often so sparse that synthetic data have to be introduced to define a circulation centre at the appropriate location. The idea is to generate a suitable high-resolution data set by simulating a tropical cyclone with the numerical model that will be used to predict the subsequent motion of storms and to use the data set as a proxy for atmospheric data. A degraded form of the model fields at an appropriate stage in the integration can be used to test a chosen analysis strategy, and an integration of the model starting from the new analysis can be compared with the control integration. The methodology has been illustrated here by calculations based on a barotropic model. The experiments described expose a range of problems that arise in trying to reconstruct a tropical-cyclone-scale vortex from sparse data. They give also an indication of the likely magnitude of track errors resulting from the sparseness of the initial data.

For the relatively narrow vortex profile studied here, which has winds higher than gale force extending 235 km from the centre, it was possible to extract the symmetric field and the vortex asymmetries from data with a resolution as low as 160 km on a regular grid. *Without* the introduction of additional data other than a knowledge of the true vortex centre, the extracted fields were accurate to within about 20% of the control fields. However, the relatively mediocre quality of the tracks at this resolution shows that 160 km is approximately a lower bound for the resolution at which a useable reconstruction of this particular symmetric vortex and its asymmetries is achievable. The best track forecasts at this resolution had 48-hour errors of up to 110 km. The threshold resolution of 160 km will presumably increase as the scale of the symmetric vortex increases. For example, it can be expected that a symmetric vortex with gale-force winds extending to 500 km can be reconstructed adequately at half the above resolution, i.e. with a regular grid size of 320 km. On the other hand, as the meteorological data are

* It should be noted that the present study only uses the information contained in the data field itself. It is hoped that the possibility of introducing synthetic asymmetries will be considered in a subsequent paper.

sampled on an irregular grid, these estimates for a proper reconstruction are certainly optimistic and are at best upper bounds of what is possible in practice.

In the medium-resolution (160 km) experiments, the accuracy with which the symmetric vortex can be recovered is greater, the closer the vortex centre is to a grid point. When the vortex centre is not close to a grid point, it is necessary to increase the strength of the analysed symmetric vortex in the inner region. A satisfactory method for doing this was to extrapolate the stream function linearly from the steepest part of the analysed symmetric profile to the vortex centre. Modification of the symmetric vortex in this way led to an improvement of the predicted vortex tracks in most of the cases investigated. However, a change of the symmetric profile alone may not improve track predictions dramatically. A faithful representation of the true symmetric profile is crucial if no information can be obtained about the asymmetries and if, for this reason, the vortex asymmetry defined in section 2(d) has to be generated artificially using the symmetric vortex. The vortex asymmetry is an important factor in vortex motion and so, therefore, is the symmetric profile used to generate it, because its structure depends on that of the symmetric vortex.

The analysis procedure applied at this resolution may be useful even when the vortex is incorrectly located in the data field. It provides a means of determining and eliminating the analysed symmetric vortex and the wave-number-one asymmetry from the field before the introduction of synthetic data to insert a correctly located vortex. This may be necessary, for example, when a radar or satellite fix shows the cyclone centre to be displaced from the circulation centre in a first guess for the analysis which is provided by an earlier model forecast. Then the vortex must be correctly relocated before an initialization of the prediction model can proceed. Even when the vortex centre cannot be located with sufficient accuracy in the analysis field, it is possible to extract at least part of the symmetric vortex before the introduction of a synthetic vortex.

With initial data at 320 km resolution it was essential to provide synthetic data to define the symmetric circulation, but even when these data were chosen with the scale and strength of the original vortex itself in mind, the symmetric vortex at the analysis time was not well captured. Moreover, the vortex asymmetry could no longer be reconstructed satisfactorily. Both the symmetric vortex and vortex asymmetry were greatly distorted by aliasing effects caused by the interpolation necessary to carry out the azimuthal analysis. This inadequate reconstruction led to significant track errors after 48 hours, even in the best case studied. In summary, if the vortex is not resolved well in the data fields, the analysed symmetric vortex may be wholly inadequate for the reconstruction of the true structure, even at large distances from the vortex centre, because of the aliasing effects mentioned above. The same is true for the vortex asymmetry.

The method devised to recover the large-scale environmental flow was found to be accurate, even at the coarsest resolution, but this may be attributable in part to the relatively large domain size compared with the scale of the vortex, and to the relative simplicity of the initially imposed environmental flow. Further tests of the scheme in more demanding situations are being carried out at present.

The new algorithm designed to determine the vortex-centre position is more accurate than simple algorithms using polynomials only, at least as long as the symmetric vortex is sufficiently well resolved in the data field, and it significantly reduces the amplitude of the spurious, neutrally stable, non-rotating wave-number-one mode that is aliased into the vortex asymmetry by an inaccurate location of the vortex centre. The performance of the birational spline interpolation scheme was found to be superior to interpolation methods using bicubic splines and algorithms incorporating approximating Bezier-splines.

As noted earlier, the interpolation with bicubic splines induces short-wave noise into the analysis which is not necessarily of small amplitude; this noise can influence the subsequent calculation of the vortex track. In contrast, an approximation with Bezier-splines alters the correct structure of the field at the original data points. The use of birational interpolating splines largely circumvents these undesirable effects.

The necessity of including synthetic data in the initial analysis in the low-resolution experiments (below 160 km for the vortex used in this study) raises a whole range of issues which we hope to address more fully in a future paper. However, it may be of interest to discuss some of these issues here. Theoretical and numerical-modelling studies have shown that, on a beta-plane, an initially symmetric vortex will not remain symmetric, even in the absence of any large-scale flow. It will generate its own asymmetries and move under the influence of these, or to be more specific, under the influence of the azimuthal wave-number-one component thereof. The present calculations show that to predict accurately the future motion of a vortex in general, a faithful representation of the large-scale flow, the symmetric circulation and at least the wave-number-one component of the asymmetries is required. Indeed, the motion of a nearly symmetric barotropic vortex can be represented by the sum of two vectors, one characterizing the motion associated with the asymmetry at the vortex centre and the other characterizing the velocity of the large-scale environmental flow at the vortex centre. With these considerations in mind, the analysis method developed in this paper suggest that an appropriate way to partition the flow in general is between the large-scale environment, the symmetric vortex, the vortex asymmetry, and the small-scale environment. The large-scale environment is defined as the lowest few wave numbers in a two-dimensional Fourier analysis, and the last three components are defined by the symmetric component, the wave-number-one component and the sum of all higher wave-number components, respectively, of an azimuthal Fourier analysis about the vortex centre.

Efforts are under way to develop further such methods for application to the reconstruction problem discussed herein. For poorly resolved data fields, neither the vortex centre, the symmetric circulation nor the vortex asymmetry can be determined with any degree of usefulness and must be either prescribed, or at least some synthetic data must be provided, so that when combined with the data that are available, the structure of these fields can be approximated.

It would be desirable to extend the methodology described in this paper to fully three-dimensional tropical-cyclone models. We believe that only in this way can the limitations of introducing synthetic data be assessed completely.

Acknowledgements

We would like to thank our colleague Dr Wolfgang Ulrich who allowed us to use his barotropic model for this study. We are grateful also to both anonymous reviewers for their most constructive comments. Finally we acknowledge financial support provided by the German Research Council (Deutsche Forschungsgemeinschaft) and the US Office of Naval Research through Grant No. 00014-90-J-1487.

References

Andersson, E. and Hollingsworth, A. 1988 'Typhoon bogus observations in the ECMWF data assimilation system'. ECMWF Tech. Memo., No. 148

Barnes, S. L. 1964 A technique for maximizing details in numerical weather map analysis. *J. Appl. Meteorol.*, **3**, 396–409

Chan, J. C. and Williams, R. T. 1987 Analytical and numerical studies of the beta-effect in tropical cyclone motion. Part I: Zero mean flow. *J. Atmos. Sci.*, **44**, 1257–1265

Davidson, N. E. and Puri, K. 1992 Tropical prediction using dynamical nudging, satellite-defined convective heat sources and a cyclone bogus. *Mon. Weather Rev.*, **120**, 2501–2522

Fiorino, M. J. and Elsberry, R. L. 1989 The role of vortex structure in tropical cyclone motion. *J. Atmos. Sci.*, **46**, 975–990

Gent, P. R. and McWilliams, J. C. 1986 The instability of barotropic circular vortices. *Geophys. Astrophys. Fluid Dyn.*, **35**, 209–233

Hovermale, J. B. and Livezey, R. E. 1977 'Three-year performance characteristics of NMC hurricane model'. Pp. 122–125 in Preprints of the 11th technical conference on hurricanes and tropical meteorology, Miami

Iwasaki, T., Nakano, H. and Sugi, M. 1987 The performance of a typhoon track prediction model with cumulus parametrization. *J. Meteorol. Soc. Japan*, **65**, 555–570

Kasahara, A. and Platzmann, G. W. 1963 Interaction of a hurricane with a steering field and its effect upon the hurricane trajectory. *Tellus*, **15**, 321–335

Kurihara, Y., Bender, M. A. and Ross, R. J. 1993 An initialization scheme of hurricane models by vortex specification. *Mon. Weather Rev.*, **121**, 2030–2045

Mathur, M. B. 1991 The National Meteorological Center's quasi-Lagrangian model for hurricane prediction. *Mon. Weather Rev.*, **119**, 1419–1447

Press, W. H., Flannery, B. P., Teukolsky, S. A. and Vetterling, W. T. 1986 *Numerical recipes*. First edition. Cambridge University Press

Reeder, M. J., Smith, R. K. and Lord, S. J. 1991 The detection of flow asymmetries in the tropical cyclone environment. *Mon. Weather Rev.*, **119**, 848–854

1992 Reply to comments of Holland *et al.*, *Mon. Weather Rev.*, **120**, 2398–2400

Ross, R. J. and Kurihara, Y. 1992 A simplified scheme to simulate asymmetries due to the beta effect in barotropic vortices. *J. Atmos. Sci.*, **49**, 1620–1628

Smith, R. K. 1993 On the theory of tropical cyclone motion. Pp. 264–269 in *Tropical cyclone disasters*. Eds. M. J. Lighthill *et al.* Peking University Press, Bejing, China

Smith, R. K. and Ulrich, W. 1990 An analytical theory of tropical cyclone motion using a barotropic model. *J. Atmos. Sci.*, **47**, 1973–1986

Smith, R. K. and Weber, H. C. 1993 An extended analytic theory of tropical-cyclone motion in a barotropic shear flow. *Q. J. R. Meteorol Soc.*, **119**, 1149–1166

Smith, R. K., Ulrich, W. and Dietachmayer, G. 1990 A numerical study of tropical cyclone motion using a barotropic model. I: The role of vortex asymmetries. *Q. J. R. Meteorol. Soc.*, **116**, 337–362

Smith, R. K., Weber, H. C. and Kraus, A. B. 1995 On the symmetric circulation of a moving hurricane. *Q. J. R. Meteorol. Soc.*, **121**, (in press)

Späth, H. 1991 *Zweidimensionale Spline-Interpolationsalgorithmen.* Oldenbourg Verlag, Munich, Germany

Ulrich, W. and Smith, R. K. 1991 A numerical study of tropical cyclone motion using a barotropic model. II: Motion in spatially-varying large-scale flows. *Q. J. R. Meteorol. Soc.*, **117**, 107–124

Weber, H. C. and Smith, R. K. 1993 The stability of barotropic vortices: Implications for tropical cyclone motion. *Geophys. Astrophys. Fluid Dyn.*, **70**, 1–30